Sustainable Energy & Fuels

# Impedance Analysis of Semiconductor Electrodes in the Accumulation Region



| | |
|---|---|
| Journal: | *Sustainable Energy & Fuels* |
| Manuscript ID | SE-ART-06-2023-000786.R1 |
| Article Type: | Paper |
| Date Submitted by the Author: | 09-Sep-2023 |
| Complete List of Authors: | Spitler, Mark; University of North Carolina at Chapel Hill, Chemistry |
| | |

ARTICLE

# Impedance Analysis of Semiconductor Electrodes in the Accumulation Region

Received 00th January 20xx,
Accepted 00th January 20xx

DOI: 10.1039/x0xx00000x

Mark T. Spitler

Given the interest in solar fuels production through electron transfer from the conduction band of semiconductor electrodes to reduce $CO_2$ or produce $H_2$, a theoretical and experimental examination has been made of these electrodes under an accumulation bias. This has been done with the use of a general model from the solid state physics literature that encompasses degeneracy situations in the electrode, a scope that is greater than the present model in use that assumes all donors are fully ionized. In an illustration of the aspects of these two models, experimental capacitance measurements with p-Si, n-Si, and n-InP have been made with a $TBAPF_6$ electrolyte in acetonitrile. A variation of the $TBAPF_6$ concentration under 0.50 M at the semiconductor electrode was used to control the capacitance of the Helmholtz layer and revealed that moderately doped semiconductors can only be biased -200 mV into accumulation before the applied potential induces band edge shifts with respect to a reference electrode. At degenerate n-InP electrodes, this shift begins at a lower potential negative of a flatband condition. The fully ionized model was found to fail with increasing bias in the accumulation region. The general model also describes expected behavior for the inversion region of these electrodes and the implications of its predictions in this regime are discussed.

## Introduction

The intent of this work is to provide a physical model for the space charge region of semiconductor electrodes employed in present research designs for solar reduction of water and $CO_2$ to produce fuel. Under a potential bias or under illumination, electrons in p-type and n-type electrodes pass from the conduction band to acceptors at the surface or in solution to effect the reductive production of energy rich products. The ability of these electrons to participate in these reactions will depend upon the energy of the semiconductor conduction band through its electron affinity as well as the potential drop across the surface Helmholtz layer when operational in an electrochemical system. Estimates of the energy of the band edges at the surface are usually made with Mott-Schottky capacitance analyses in the depletion region of the semiconductor, which assumes that all dopants in the semiconductor are ionized. [1]

These estimates of the potential of the conduction band edge $E_c$ and the valence band edge $E_v$ are made in the depletion region of the semiconductor electrode, whereas all fuel-producing designs with n-type or p-type semiconductors operate with semiconductors with bands flat or in possible accumulation or inversion regimes where not all dopants are fully ionized. There is a lack of physical models for the space charge regime that will help guide research under these conditions.

This work will provide a general physical model that describes accumulation and inversion at uniformly doped semiconductor electrodes and will support them with experiment in the accumulation regime. In order to do this, it was necessary to revisit the original solid-state literature and find physical models that could describe degeneracy in the bulk or in the space charge region, where metallic conductivity is attained for majority or minority carriers or not all dopants are ionized. The derivations here are classical in nature and avoid consideration of quantized energy levels for charge carriers at the surface, but the experimentation does provide some insight into this possibility.

[a] Department of Chemistry, Campus Box 3290, University of North Carolina at Chapel Hill, Chapel Hill, NC 27599-3290, USA

† The corresponding author is a Visiting Scholar at the University of North Carolina. E-mail: spi1tlerm@email.unc.edu

Electronic Supplementary Information (ESI) available: [Experimental data for analyses of capacitance measurements]. See DOI: 10.1039/x0xx00000x

To provide a context for the introduction of this general model that includes degeneracy, it is necessary to summarize the physical principles behind Mott-Schottky plots of capacitance. This will allow a parallel and truncated derivation of a general model as well as the use of a common terminology to aid in interpretation of experimental work in the accumulation region.

Capacitance measurements have commonly been employed in semiconductor electrochemistry to determine the flat band potential, $V_{fb}$, of semiconductor electrodes in solution in order to obtain potentials for the conduction band Ec and valence band Ev. This technique was first introduced by DeWald[2, 3] in examinations of ZnO electrodes. With the measurement of the capacitance C for an electrode biased in the depletion region of the semiconductor, one can extrapolate to the potential where the bands of the semiconductor are flat, to where the electric field within the space charge region is zero. Many examinations of the utility and validity of this approach can be found in the literature.[4-6]

The well-known form of this expression for an n-type electrode is:[2, 3]

$$\frac{1}{C^2} = \left(\frac{2}{eN_D \epsilon \epsilon_0}\right)\left(V_{appl} - V_{fb} - kT/e\right) \quad (1)$$

where e is the unit charge, $\epsilon$ is the dielectric constant of the material, $\epsilon_0$ is the permittivity of free space, and $N_D$ is the doping density of donors in the solid. A plot of experimentally measured capacitance against the applied potential $V_{appl}$ is commonly used to determine $N_D$ from its slope and the Mott-Schottky intercept $V_{fb}$ on the potential axis.

This expression for capacitance was derived from early semiconductor physics research by Schockley and Garrett and Brattain in the 1950s.[7, 8] Out of this early work came mathematical expressions describing the charge and electric field of a semiconductor space charge region which made it possible to calculate the surface charge carrier concentration of a semiconductor under bias. The derivations relating to the depletion region of a semiconductor are summarized in the Supplementary Information **S1** S2**.**

However, there are two immediate aspects of the derivation of eqn (1) that are little appreciated and are worthy of mention before turning to a physical description of an accumulation layer. The first concerns the "flat band" potential intercept $V_{fb}$, which eqn (1) shows is kT away from the potential where the sum of all charges from electrons, holes, and ionized dopant atoms equals zero. For an electrode in the dark and without redox couples in the electrolyte, this implies that the bands are flat. However, in the presence of redox couples or under illumination where mobile carriers have been injected into the space charge region, Mott-Schottky analyses following eqn (1) yield an intercept with the potential axis only where there is zero net charge and not necessarily where the bands are flat. The injected charge plays a role. (**SI** eqn (4s)) A second observation from the derivation of eqn (1) is that at $V_{fb}$ -$kT/e$ = 0, the capacitance of the space charge region $C_{SC}$ is given by:

$$C_{sc} = \sqrt{2}\left(\frac{e^2 N_D \epsilon \epsilon_0}{2kT}\right)^{1/2} \quad (2)$$

(**SI** eqn (4s)) This self-consistency check is rarely used in the literature. It assumes that any potential drop of the applied potential across the Helmholtz layer and electrolyte can be neglected.

In this work, accumulation and inversion space charge regions are examined to give information about semiconductor electrodes that these depletion region analyses cannot provide.

In doing this, the physics must consider circumstances where the dopants in the semiconductor are not fully ionized, where degeneracy can occur. This can be a bulk phenomenon where degenerate semiconductors are examined, but it would be more commonly encountered by the experimentalist with doped semiconductor electrodes biased to create an accumulation region where the fermi level, or electrochemical potential, falls between the potential of the dopant level and the band populated by dopant atoms that happen to be ionized. Proper treatment of this problem also allows a picture of inversion regimes for a semiconductor electrode as well.

A full derivation that treats degeneracy in a semiconductor was developed contemporaneously with Garrett and Brattain[7] and results in the following expression corresponding to eqn (2) for the electric field E of the space charge region:[9]

$$E = \mp \frac{kT}{e\mathcal{L}_D}\left\{\begin{array}{c} \frac{N_D}{n_i} ln\left[\frac{1+\frac{1}{2}\exp\left(w_{D,I}-u_s\right)}{1+\frac{1}{2}\exp\left(w_{D,I}-u_B\right)}\right] + \\ \frac{N_A}{n_i} ln\left[\frac{1+\frac{1}{2}\exp\left(u_s-w_{A,I}\right)}{1+\frac{1}{2}\exp\left(u_B-w_{A,I}\right)}\right] - \\ \frac{1}{F_{1/2}(w_{V,I})}\left[\frac{2}{3}F_{\frac{3}{2}}(w_{V,I}-u_B) - \frac{2}{3}F_{\frac{3}{2}}(w_{V,I}-u_S)\right] + \\ \frac{1}{F_{1/2}(w_{I,C})}\left[\frac{2}{3}F_{\frac{3}{2}}(u_S-w_{C,I}) - \frac{2}{3}F_{\frac{3}{2}}(u_B - w_{C,I})\right] \end{array}\right\}^{1/2} \quad (3)$$

where $\mathcal{L}_D = \left(\epsilon\epsilon_0 kT/2e^2 n_i\right)^{1/2}$ is the Debye length and $n_i$ is the intrinsic carrier density. The remaining terms are depicted in Fig. 1 as: $u_b = e(E_f - E_i)/kT$, $E_i = (E_c + E_v)/2$ , $u_s$ is $u_b$ at the surface, $E_D$ and $E_A$ are the donor and acceptor energies, $w_{X,Y} = (E_X - E_Y)/kT$. $N_A$ represents the number of acceptor dopants. The function F is the Fermi-Dirac integral given in the form of:

$$F_{1/2}(\eta) = \int_0^\infty \frac{x^{1/2}dx}{1+\exp\left(x-\eta\right)} \quad (4)$$

Here $x = (E-E_C)/kT$ for an n-type semiconductor and $x = (E-E_V)/kT$ for a p-type semiconductor. The same result is obtained using the more versatile script form $\mathcal{F}j(\eta) = \frac{2}{\pi}F_j(\eta)$. Under the degeneracy regimes that eqn (3) governs, the position dependent potential in the space charge region is obtained through the integration of eqn (3) over distance.

An energy level diagram for this expression is found in Fig. 1 where both solid-state physics and electrochemical sign conventions are shown. At the time that eqn (3) was developed in 1958 it was too tedious to calculate an exact evaluation in all of its applications given the limits of available computational techniques. Only occasionally does one encounter its use, and that in limits and approximations.[10] Presently, it can be evaluated with several lines of commercial computational software.

This work will proceed first with a derivation of a capacitance expression for the general model from eqn (3). It will then illustrate the predictions of this model with experimental capacitance measurements of p-Si and n-Si electrodes biased in accumulation where degeneracy should be encountered in the space charge region. To illustrate the impedance properties of a degenerate material, n-InP will be examined in this study as well. Mott-Schottky analyses have been reported in the literature for n-type InP revealing a doping density of $10^{18}$/cc – $10^{19}$/cc.[11] Given the low effective mass of electrons in InP of .08 $m_e$, the density of states of the InP conduction band can be calculated to be $6x10^{17}$/cc. Thus, such past study has been made with degenerate material. This implies that the full model of eqn (3) must be used to obtain an accurate behavioral description for n-InP electrodes with the commonly encountered dopant levels of this solid. The limitations of the fully ionized model of eqn (3) will then be quantified relative to this general model. It is also possible that the potential in an accumulation bias can be so large and steep in form within and the space charge region so narrow in dimension that quantization of charge carriers occurs. Seiwatz and Green expressed such a caveat in their original work.[9] This possibility has been the focus of later research[12, 13] and the use of eqn (3) will allow further insight on this area for the electrodes under investigation. In conclusion the expected characteristics of inversion regions will be discussed given the observed behavior for these solids in accumulation.

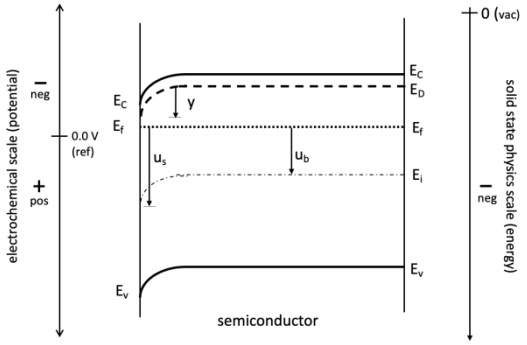


**Fig. 1** An energy level diagram is given for an n-type semiconductor under accumulation. From a solid state physics perspective all energies are negative with respect to vacuum. The electrochemical signs are taken with respect to a reference electrode where there is both a negative and a positive sign to potentials. $E_C$, $E_f$, $E_i$ ,$E_D$, and $E_V$ represent the energies of the conduction band edge, the fermi energy, the intrinsic band gap center, the donor level and the valence band edge. $y_s$ is shown to be the band bending and $u_b$ and $u_s$ are variables in the solid state physics formulation of the general model of eqn (6).

## Experimental

Silicon, both n- and p-type, and n-type indium phosphide electrodes were made from wafers of these materials. The silicon was obtained from NOVA Electronic Materials with the InP being Crysta-Com material. These wafers were single-side polished with electrical contacts being made to the rough, back side. The p-type Si, boron doped, was oriented with the <111> orientation and was reported by the vendor to have a resistivity of 1-20 ohms. The phosphorous doped n-type Si was obtained with a polished <111> surface and had a 30 ohm resistivity. The polished InP surfaces were <110> in orientation. Doping of the crystals was with Sn for the n-type samples with a doping level of ~$10^{17}$/cc having been provided by the vendor.

Prior to measurement, the polished surfaces were exposed to in a piranha etch (3:1 $H_2SO_4/H_2O_2$) for 30 min, They were then rinsed with $H_2O$ and dried under a stream of $N_2$ and then etched in HF for 40 s using a buffered oxide etchant (10:1) with >5% HF. Following the etch, the surface was washed with water, acetone and then dried under a $N_2$ stream. Ohmic contacts were made by scoring the unpolished side of the Si with a diamond-tipped scribe and rubbing with GaIn eutectic. Contact to the electrodes was made with either conductive Cu tape or conductive silver epoxy to a copper wire. InP electrodes ranged in size from 0.050 $cm^2$ to 0.50 $cm^2$ in size and contacted in the same manner as the Si electrodes. Prior to use, they were etched for 45 sec in a methanol solution of 2% $Br_2$.

Electrochemical measurements were made at room temperature in spectrochemical grade acetonitrile using tetrabutylammonium hexafluorophosphate ($TBAPF_6$) from Fluka which had been recrystallized three times before use. These measurements included current-voltage curves, impedance measurements as a function of potential and plots of the frequency dependence of the impedance at set bias potentials over the range of 10 Hz to $10^5$ Hz. Experimentation with the electrodes was performed in a custom-built electrochemical cell with electrolyte solutions that had been bubbled with $N_2$ for twenty minutes. In the case of n-type Si electrodes immersed in low, 1 to 100 mM electrolyte solutions, the assembly of the cell and measurements were made in an inert $N_2$ filled atmosphere glovebox in which the electrolyte was made with acetonitrile that had been dried to 1-2 ppm of water. A Pt mesh electrode served as the counter electrode with an SCE reference that was calibrated against ferrocene. A CH Instruments 760 potentiostat was employed in this work. Given the steep dependence of the impedance upon potential in these experiments, the modulation amplitude was held to 5 mV.

## Results

Capacitance measurements have been made with Si and InP semiconductor electrodes in acetonitrile biased over the depletion and accumulation regions. In order to obtain a continuous physical treatment of the electrode capacitance applicable to this range, one must derive an expression for the expected experimental capacitance from the electric field expression of eqn (3). In parallel with the derivation of eqn (1) we have:

$$C_{SC} = = \left(\frac{e^2\epsilon\epsilon_0 n_i}{2kT}\right)^{1/2} \times$$

$$\left\{\begin{array}{l} -\frac{N_D}{n_i}\left[\frac{1}{1+2exp(u_s-w_{D,I})}\right]+\frac{N_A}{n_i}\left[\frac{1}{1+2exp(w_{A,I}-u_s)}\right] \\ -\frac{1}{F_{\frac{1}{2}}(w_{V,I})}F_{\frac{1}{2}}(w_{V,I}-u_s)+\frac{1}{F_{\frac{1}{2}}(w_{I,C})}F_{\frac{1}{2}}(u_s-w_{C,I}) \end{array}\right\}/(\mathrm{Z})^{1/2}$$

(5)

Z represents the terms within the brackets of eqn (3). This is a general expression for capacitance that covers the range from degenerate to non-degenerate semiconductors, both n- and p-type. It covers inversion regions as well as depletion and accumulation. There have been prior approximations to eqn (5),[14] where the first dopant terms in eqn (3) have been omitted, but an accurate description of the transition from depletion to accumulation requires their inclusion.

As mentioned above, degeneracy is most often encountered by the experimentalist in the space charge region when an electrode is biased at a potential where the fermi level is within kT of the energy of the dopant atom, negatively biased for an n-type semiconductor and positively for a p-type electrode. The semiconductor could also be degenerate in the bulk. In the case of a n-type semiconductor when $E_D$-$E_f$ < 2kT in a solid state sense, when the fermi level is near or negative of the energy of the donor state, not all of the donors are ionized. This is a regime that is avoided in impedance analyses in semiconductor electrochemistry and is new to the discussion. In this situation, a Boltzmann expression cannot be used to calculate the position of the fermi level at flatband from the doping density. One must make use of a neutrality condition at flatband that employs the full Fermi function to describe population statistics. Taking an n-type semiconductor at $y_s = 0$ where $N_A$ is zero and the intrinsic hole concentration is negligible, the positive charge from the ionized donor species should be equal to the number of electrons in the conduction band of the semiconductor, as given by:

$$\frac{N_D}{(1+2\exp(u_b - w_{D,I}))} =$$

$$\mathcal{D}(E_c)\frac{2}{\sqrt{\pi}}F_{\frac{1}{2}}(u_b - w_{C,I}) = 2\left[\frac{2\pi m_{n*}kT}{h^2}\right]^{3/2}\frac{2}{\sqrt{\pi}}F_{\frac{1}{2}}(u_b - w_{C,I}) \qquad (6)$$

Here the effective mass of the electron for the solid is $m_{n*}$and h is Planck's constant. $\mathcal{D}(E_c)$ is the conduction band density of states. For a given Fermi level expressed as $u_b = (E_f - E_i)/kT$, eqn (6) allows determination of $N_D$. A corresponding expression can be made for degenerate p-type semiconductors.

In the limit where donors are fully ionized, it can be shown that the expression of eqn (5) (**SI** S3) reduces mathematically to eqn (1). The numerical evaluations match as well. In the limit where $y_s$ approaches zero, eqn (5) reduces to the expression of eqn (2).

Deviations of eqn (5) from the fully ionized assumption of eqn (1) begin when the bulk semiconductor approaches degeneracy in doping. A comparison has been done in Fig. 2 for n-Si electrodes where model capacitance-potential curves have been calculated for low-doped, $5x10^{14}$/cc and higher doped, $6x10^{17}$/cc material. Here solid lines describe the capacitance for a doping of $5x10^{14}$/cc. They are shown as a function of $y_s$ in the semiconductor at potentials from far negative to far positive of $y_s = 0$, from accumulation to inversion. These curves contrast with the capacitance predicted by the fully ionized dopant approach that leads to eqn (1). The latter function increases exponentially, as would be expected for a model based upon a Boltzmann population of the bands. The general model of eqn (5), however, begins to level off at extreme potentials because its physics makes use of the fermi function to determine carrier concentrations in the bands. It should be noted that the existence of an inversion region is dependent upon a source of

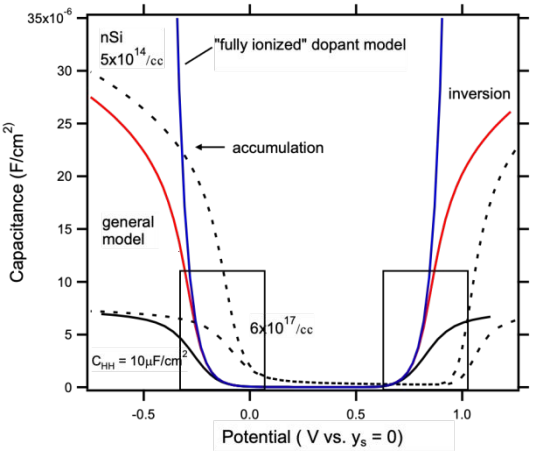


**Fig. 2** A comparison is made of the capacitance of a space charge region for n-Si doped at $5x10^{14}$/cc which shows the general model of eqn (5) and the fully ionized dopant model of eqn (1). Both accumulation and inversion regions are shown. Using the general model, the capacitance of a higher doping density of $6x10^{17}$/cc for n-Si is also shown as a dashed curve. When the n-Si is employed as an electrode in an electrochemical cell with a Helmholtz layer capacitance of 10 μF/cm², the electrode capacitance is calculated to plateau at a low level between 5 and 10 μF/cm².

carriers to populate the appropriate minority band which may be possible with redox agents in solution or illumination. Otherwise, only a deep depletion region would be observed.

Also shown in Fig. 2 is the prediction of an experimental measurement of the capacitance for both n-Si doping densities when the capacitance of the Helmholtz layer $C_{HH}$ is taken to be $10^{-5}$ F/cm², which is a typical value for the double layer at a metal electrode. These projected measured system capacitances $C_{meas}$ are derived from the series expression for two capacitors:

$$\frac{1}{C_{meas}} = \frac{1}{C_{sc}} + \frac{1}{C_{HH}} \qquad (7)$$

The potential scale for this particular curve in Fig. 2 is taken to be the applied potential $V_{appl}$, containing the sum of potential drops across the semiconductor and the Helmholtz layer which is derived from eqn (7). It is clear that within a few hundred millivolts negative of the onset of accumulation or inversion, a plateau is reached, implying that $C_{meas}$ is dominated by the $C_{HH}$ term and an unpinning of the semiconductor bands occurs where the potential of the band edges, be it $E_c$ or $E_v$, shifts with respect to a reference electrode in solution. In this case, a significant fraction of the applied potential drops across the Helmholtz layer, a fraction that can be calculated if $C_{HH}$ is known.

Experimentally such plateaus are observed in this work for the measured impedance of semiconductor electrodes when biased in the accumulation region. This will be shown first for p-Si. Capacitance measurements were performed on p-Si in acetonitrile with several different $TBAPF_6$ concentrations as the electrolyte solution with a potential bias that ranged from the depletion regime into accumulation.

The data are given in Fig. 3 with the impedances being analyzed using the equivalent circuit in the inset. Mott-Schottky analyses were made of these impedance curves in the depletion region with an average $V_{fb}$ being found of -.61 vs ferrocene and

an average doping density $N_A$ of $5x10^{15}$/cm$^2$ being derived. (**SI** Fig. S1) From $V_{fb}$ and eqn (1), the potential for zero band

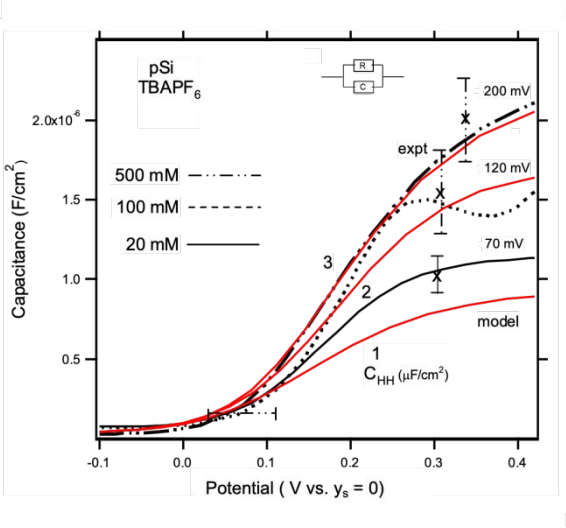


**Fig. 3** The capacitance $C_{meas}$ of a $4x10^{15}$/cc doped p-Si electrode in a $TBAPF_6$/acetonitrile electrolyte was measured as a function of the $TBAPF_6$ concentration from 20 mM to 500 mM. Selected curves are shown for each level where their abscissas have been shifted to align their Y = 0 potentials. It is seen that in a negatively biased accumulation region a plateau in $C_{meas}$ is reached that increases with concentration. Vertical error bars show the range of the plateau levels observed; the horizontal bar shows the range in measured $V_{fb}$ potentials. Solid curves represent model capacitance behavior from eqn (5) and eqn (7) for $C_{HH}$ values of 1, 2, and 3 x$10^{-6}$ F/cm$^2$. Further analyses provides the upper limits to Y which are listed above each curve at 0.4 V.

bending, $y_s$ = 0 could be found. Only those results were considered where $V_{fb}$, $y_s$ = 0, and $N_A$ were internally consistent with eqn (2) to within 2kT. The results for 20 mM, 100 mM and 500 mM electrolyte are shown in Fig. 3 where the potential of the experimental curves have been shifted to a common $y_s$ = 0 value. Each curve is a representative selection from five to ten experiments, with the error bars in Fig. 3 being the standard deviation about the average. A plateau is observed for each case and the average values for each electrolyte concentration are separated distinctly from the others. Plateaus for 20 mM, 100 mM, and 500 mM $TBAPF_6$ are found at 1.1 x $10^{-6}$, 1.7x$10^{-6}$, and 2.4x$10^{-6}$ F/cm$^2$. In changing [$TABPF_6$] and not the electrode material in these experiments, it is concluded that these changes in the saturation capacitances in accumulation result from changes in the Helmholtz layer. The plateau values of the capacitances are then taken to represent the $C_{HH}$ as a function of [$TBAPF_6$] and in this region it is expected that any change in $V_{appl}$ will fall predominately across the Helmholtz layer.

Experimentally it was found that polarization of the electrode much more positive than the onset of the plateau could cause the observed impedance curve to change its shape or saturation value in any immediate subsequent measurements. The curvature in the 100 mM $TBAPF_6$ result is an example. Such curvature can be found in the literature for semiconductor electrodes.[15] In several experiments with p-Si, the potential range of these capacitance measurements was extended to regions where Fig. 2 would predict an inversion region to be found, as negative as -1.4 V vs. ferrocene. Yet, depletion region behavior is still observed (**SI** Fig. S1a), implying

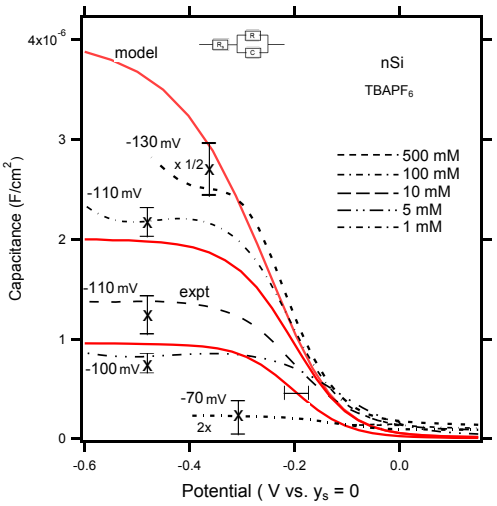


**Fig. 4** The capacitance $C_{meas}$ of a $4x10^{15}$/cc doped n-Si electrode in a $TBAPF_6$/acetonitrile electrolyte was measured as a function of the $TBAPF_6$ concentration from 1 mM to 500 mM. Selected curves are shown for each level where their abscissas have been shifted to align their Y=0 potentials. It is seen that in a negatively biased accumulation region a plateau in $C_{meas}$ is reached that increases with concentration. Vertical error bars show the range of the plateau levels observed; the horizontal bar shows the 50 mV range in measured $V_{fb}$ potentials. Solid curves represent model capacitance behavior from eqn. (5) and eqn (7) for $C_{HH}$ values of 1, 2, and 4 x$10^{-6}$ F/cm$^2$. Further analyses provides the upper limits to Y which are listed above each curve at -0.6 V.

the presence of deep depletion in the space charge region, where the negative charge of the applied bias is in part manifest as negatively charged acceptor dopants in the bulk.

With the conclusion that the impedance at these plateaus represent $C_{HH}$, model curves were calculated for this doping level of p-Si from eqn (5) and eqn (7) for $C_{HH}$ values of 1, 2, and 3 x $10^{-6}$ F/cm$^2$ and are shown in Fig. 3. The onset and shape of the experimental curves compare well with the model predictions and they almost overlap for the 500 mM case.

Follow-up measurements to support these observations were done with n-Si in a nitrogen glove box at electrolyte concentrations down to 1 mM where a diffuse double layer is expected.[13] The intent is to distinguish the double layer impedance effects from possible surface layers on the electrode formed electrochemically or thermally. Under nitrogen with single ppm dry acetonitrile, impedance measurements on n-Si were recorded for 1 mM, 5 mM, 10 mM, 100 mM and 500 mM $TBAPF_6$ with the results being given in Fig. 4. They were analyzed with the equivalent circuit in the inset of Fig. 4, where the solution resistance Rs is taken from a Nyquist plot of the data. The average doping density $N_D$ was found to be $2x10^{14}$/cc with a $V_{fb}$ of -. 40 vs ferrocene. (**SI** Fig. S2)

The results are shown in Fig. 4 for the several concentrations of electrolyte where the potential of each experimental curve has been set to zero at its $y_s$ = 0 value. Only internally consistent Mott-Schottky results according to eqn (2) were considered. Each curve is a representative selection from the experimental results, with the average and standard deviation of the plateau value being given for each concentration.

The average plateau values for impedance at each concentration are seen to be distinct from each another and to range from .2 to 5.8 x $10^{-6}$ F/cm$^2$. This thirty-fold range in

saturation impedances supports the conclusion that the observed capacitances are controlled by the Helmholtz and diffuse layers at the interface. As with the p-Si results of Fig. 3, model curves were calculated for the doping density of n-Si for 1, 2, and 4 x$10^{-6}$ F/cm$^2$ and are given in Fig. 4 for comparison.

Impedance measurements of n-InP were made in 100 mM $TBAPF_6$ in acetonitrile over a potential range from the depletion region and into accumulation. Mott-Schottky analyses with data from the depletion region yielded a doping density of 6 (+/- 1) x$10^{17}$/cc and $V_{fb}$ values of -1.15 V vs. ferrocene. (**SI** 4c)
A representative result is given in Fig. 5 with its measured bias potential set to zero where $y_s$ =0. Model curves derived from eqn (5) and eqn (7) are also shown in Fig. 5 for doping densities of $10^{15}$/cc, $10^{16}$/cc, $10^{17}$/cc, and $10^{18}$/cc.

## Discussion

The capacitance-voltage curves in Fig. 3 and Fig. 4 for p-Si and n-Si all reach a plateau value for capacitance in the accumulation region that varies with the electrolyte concentration. As the $TBAPF_6$ concentration in the acetonitrile electrolyte is dropped from 500 mM to 1 mM, this plateau falls with saturation values from 5x$10^{-6}$ F/cm$^2$ down to 2x$10^{-7}$ F/cm$^2$. At a metal electrode this would represent a transition from a compact Helmholtz layer at the surface at 500 mM to a diffuse double layer below 10 mM.[16] Pragmatically, the importance of the diffuse double layer in this work is only its capacitance relative to that of the semiconductor space charge region under bias. Compared with the theory and experiment on diffuse double layers at metal electrodes, the role of diffuse double layers at semiconductor electrodes is unknown. With an accurate model for band bending and charging of the semiconductor such as given in eqn (3) and eqn (5), it now becomes possible to distinguish semiconductor contributions to the capacitance from solution contributions and to begin to analyze the role of a diffuse layer at semidconductor electrodes.

With the conclusion that the observed plateaus in the impedance measurements represent the term $C_{HH}$ for the particular system under study, it is clear that through the use of eqn (7) that these $C_{HH}$ plateau values can be used to extract $C_{SC}$ from $C_{meas}$ at each bias potential in the experimental curves of Figs 3 through 5. They allow one to evaluate the partition of the potential drop across the interface into separate space charge and Helmholtz/diffuse layer components.

Making use of the plateau values for $C_{HH}$, the parameters of the semiconductor half of the interface, $C_{SC}$ and $y_s$, are calculated for the experimental p-Si curves of Fig. 3. With this information, the value of $V_{appl}$ can be determined for the curves in Fig. 3 where $E_f = E_c$. Given the doping density of this electrodes of 4x$10^{15}$/cc, $E_f$ at $y_s$ = 0 is 200 mV positive of $E_c$ and a negative band bending of this value would be necessary for $E_f$ to equal $E_c$. However, with $C_{meas}$ limited to the plateau values of these curves and corresponding to $C_{HH}$, it is calculated with the aid of eqn (7) that $y_s$ levels out at negative polarizations and reaches only 200 mV with the 500 mM electrolyte and only with a bias of -400 mV. As [$TBABPF_6$] falls from 100 mM to 20 mM the limit was found to fall from 120 mV to 70 mV which is negative of $E_f = E_c$, where the balance of any further applied potential falls across the Helmholtz layer. The calculated limiting $y_s$ values are given above the curves in Fig. 5 at a $V_{appl}$ of -400 mV.

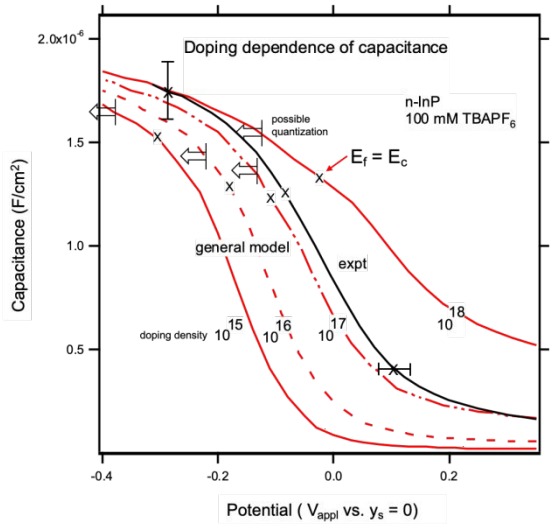


**Fig. 5** An experimental capacitance measurement is shown for the near degenerate n-InP electrodes in a 100 mM $TBAPF_6$ electrolyte with a derived doping density of 6x$10^{17}$/cc. With it are shown predictions from the general model of eqn (5) for a $C_{HH}$ of 1.8x$10^{-6}$ F/cm$^2$ and doping densities that vary from $10^{15}$/cc to $10^{18}$/cc, the last doping exceeding the conduction band density of states of 7x$10^{17}$/cc. For each curve, the potential at which $E_f = E_c$ is marked with an "X." The range in $V_{fb}$ and the observed plateaus for measurements are given by error bars. Arrows represent potentials for each doping density where the band bending at the surface changes by kT within the Debye length of the electron and quantization becomes possible.

The further examination of this behavior made with n-Si electrodes at electrolyte concentrations from 500 mM down to 1 mM revealed plateau values were observed in these cases as well. They also fell with decreasing electrolyte concentration. In a manner similar to the p-Si analyses, the plateau values were taken to represent $C_{HH}$ values for the electrode allowing the limiting $y_s$ values for the electrodes in accumulation to be determined. For the lower doped n-Si material of 2x$10^{14}$/cc, the $E_C$-$E_f$ difference at $y_s$ = 0 is determined to be 280 mV. As listed at the left side of Fig. 4 above the experimental curves, the limiting $y_s$ values are -130 mV or smaller. This situation for n-Si is a downwards band bending as depicted in Fig. 1 with the limits revealing that this bending never reaches the point where $E_f = E_c$.

The experimentation with n-InP was done to illustrate behavior where degeneracy occurs in the bulk as well as in the space charge layer. In Fig. 5, the calculated capacitance curve for $10^{15}$/cc n-InP electrodes is similar in form to the similarly doped n-Si curves of Fig. 3. A $C_{HH}$ of 4x$10^{-6}$ F/cm$^2$ was assumed in the calculation. For this low doped n-InP calculation, $y_s$ becomes negative enough in the accumulation region for $E_f$ to equal $E_c$ within 300 mV negative of $y_s$ = 0, as marked on the plot. As the doping increases, the potential in the accumulation region where $E_f = E_c$ shifts to more positive potentials and at $10^{18}$/cc, higher than the conduction band density of states $\mathcal{D}(E_c)$ of 6x$10^{17}$/cc, it appears coincident with $V_{fb}$. The experimental curve falls between $10^{17}$/cc and $10^{18}$/cc and describes the same form as the model curves. At a $V_{appl}$ more negative than these marked potentials, any additional polarization falls mainly across the Helmholtz layer.

In an illustration of this behavior, Fig. 6 shows the fraction of $V_{appl}$, $\gamma_{ac}$, to use the terminology of earlier work,[17] that falls

across the Helmholtz layer with a change in $V_{appl}$ for each potential in the experimental curves of n-Si and n-InP from Fig. 4 and Fig. 5. This was also done with eqn (5) and the observed plateau $C_{HH}$ levels. Although band edge shifts of the

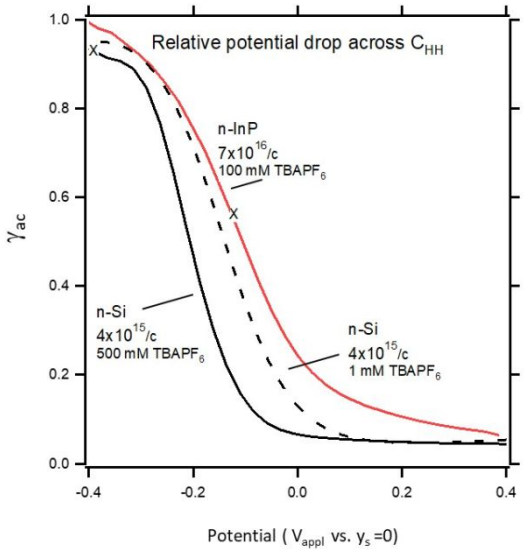


**Fig. 6** The per cent of $V_{appl}$ that falls across the Helmholtz layer with a change in $V_{appl}$ is given for each potential for experimental curves of n-Si and n-InP from Fig. 4 and Fig. 5. For the n-Si, the potential drop across the Helmholtz and diffuse layers per unit change in $V_{appl}$ exceeds 50% within a 200 mV negative bias of Y=0 and the band edges of the Si electrodes shift significantly with respect to a reference electrode. The highly doped InP begins a shift even positive of Y=0 and $V_{fb}$. The potential at which $E_f = E_c$ is marked with an "X."

semiconductor with bias are seen through Fig. 6 to occur at a very low levels in the depletion region, at a 200 mV bias negative of $y_s$ = 0, the band edges of the n-Si electrodes have shifted significantly with respect to a reference electrode. The fraction increases from 0.4 at 500 mM electrolyte concentration to 0.7 for 1 mM. To hold $E_c$ near a specific potential value against an external reference, it is apparent that one must work at high electrolyte concentrations. This would be found in any semiconductor electrode system for reduction of $CO_2$ or production of $H_2$ at a typical current flux of 10 mA/cm$^2$ because of the amount of charged by-products produced in these reduction reactions without regard to the amount of any added electrolyte. However, even at high electrolyte concentration, the band edges will begin to shift at one point because the model curves in Fig. 2 rise very sharply within several hundred millivolts of the onset of inversion or accumulation.

Given this observation for these n-type electrodes, it is evident that electron transfer to or from the conduction band near $y_s$ = 0 occurs at $E_c$ values that shift with the conditions of the experiment, and these include electrolyte concentration and semiconductor doping density. The use of Mott-Schottky analyses to determine $V_{fb}$ and therefore $E_c$ from behavior in the depletion region is therefore only crudely approximate. However, the deviations from the real $E_c$ in operational systems in terms of doping density and electrolyte still remain under the control of the experimentalist.

It is within the potential range of the outlined boxes of Fig. 2 that the fully ionized model ceases to be a good description of the space charge region. When the curves for accumulation and inversion are expanded (**SI** Fig. S4) the ratios of the fully ionized model to the general model rise steeply within 100 mV of the bias where $E_f$ equals $E_C$ or $E_V$. The fully ionized model of eqn (1) ceases to be a good description of the band bending in the semiconductor. This is found for the InP electrodes (**SI** Fig. S5), but not here for Si owing to low $C_{HH}$ values.)

With the aid of eqn (3) it is possible to determine the potential for onset of charge quantization in the accumulation region of the Si and InP semiconductor electrodes of this study. Quantal behavior in this regime has been a subject of interest in the past and it requires that the potential change of the bands at the surface equal or exceed kT within the Debye length of the electron or hole. Using a Debye length for the charge carriers of 1 to 5 nm (**SI** eqn S8), and the electric field at the surface from eqn (3) and with the use of eqn (5) the prediction is that a band bending $y_s$ of 180-280 mV is required to meet the kT minimum requirement for the p-Si of Fig. 3. Similarly, a $y_s$ of 150 mV holds for the n-Si experiments of Fig. 4. For the electrolyte, doping densities and polarizations of the electrodes in these experiments, only the 500 mM p-Si comes close to meeting the quantization criterion. A different result is predicted for InP with its much lower effective mass and a Debye length several times greater. Marked in Fig. 5 are the experimental potentials of the model curves from $10^{15}$/cc to $10^{18}$/cc in doping at which the minimum quantum criterion is met. At these potentials and more negative, an accurate description of behavior cannot rely solely upon a classical model.

Both models predict an increase in capacitance of the semiconductor electrode in inversion, but experimental measurements in this region are beyond the scope of this work. They would be much more complex in design. It is expected, however, that curves similar to that of Fig. 3, Fig. 4 and Fig. 5 would result. Owing to the high value of $C_{SC}$ near the band edge shown in Fig. 2 for inversion, $C_{HH}$ would dominate the $C_{meas}$ and a plateau would result.

The theoretical calculations assume that the charge in the space charge region in inversion is described by the equilibrium expression of eqn (5) and for a p-type material is attributable solely to electrons in the conduction band at the surface. However, the electron population of any inversion region for p-Si in the dark and without redox couple would be a dynamic balance between supply of electrons from the bulk and loss through reduction of any adventitious solution species.

The steady state electron density at the surface appears to be below the equilibrium level. This is supported by the observation that only depletion behavior was observed experimentally in the capacitance of p-Si polarized to -1.4 V where inversion should occur. This implies that ionized dopants contribute to the charging of the space charge region and it is likely that the charge is partitioned between a depletion region and a small thin region of inversion where a small steady state concentration of electrons at the surface can also exist. Fig. 2 shows the high capacitance of an inversion region in comparison with the low capacitance of a depletion region. The interface could then be seen as a series sequence of a small inverted region and a much larger depletion region where the capacitance of the latter should be much smaller than that of the former. In an impedance measurement therefore, only the depletion region would be measurable. Only when the inversion

region is fully populated according to eqn (5) would it dominate any measured impedance. Therefore, some steady state concentration of electrons should be present, but very small. In non-equilibrium, steady state situations such as this, more direct probes of electron concentration at the surface are required to detect inversion.

The inversion region could be populated at high levels through p/n (or n/p) junctions beneath the electrode/electrolyte interface where minority carriers would be injected across the junction into the electrode. This would be a clean approach. It could also be done through photoexcitation of the solid with bandgap radiation or the inclusion of redox couples in the solution. In these latter situations, however, it would be necessary to account for both the electron and hole concentrations in the space charge region (**SI** eqn (4s)) and, as mentioned, this must be done in a numerical simulation of charge concentrations at the electrode surface and their creation and destruction.

## Conclusions

A physical model has been developed that describes the equilibrium behavior of semiconductor-electrolyte behavior in inversion and accumulation as well as degenerate semiconductors. However, in the presence of redox couples or illumination, a numerical approach may be required to obtain a picture of ideal behavior.

Experimental capacitance measurements for p-Si and n-Si show that for [$TBAPF_6$] below 0.5 M, the diffuse double layer plays a role and band bending in accumulation is limited to 200-300 mV before band edge shifts with respect to solution occur.

Even above 0.5 M such a band edge shift will eventually occur with increasing polarization. Similar behavior is expected for inversion layers at equilibrium, but experimental systems at inversion appear to operate at a steady state to produce an interface where impedance techniques have limited sensitivity.

## Conflicts of interest

There are no conflicts to declare;

## Acknowledgements

The author wishes to acknowledge the support of the UNC Chemistry Department in the execution of this research. A portion of this work was performed using the Anaerobic Glove Box Environments in the CHASE Hub Instrumentation Facility, Solar Fuels Product Analysis Laboratory, established by the Center for Hybrid Approaches in Solar Energy to Liquid Fuels (CHASE), an Energy Innovation Hub funded by the U.S. Department of Energy, Office of Science, Office of Basic Energy Sciences under Award Number DE-SC0021173.

## References

(1) Memming, R. *Semiconductor Electrochemistry, 2nd Ed.*; WILEY-VCH Verlag GmbH, 2015.
(2) Dewald, J. F. The Charge and Potential Distributions at the Zinc Oxide Electrode. *Bell System Technical Journal* **1960**, *39* (3), 615-639.
(3) J.F., D. Charge Distribution at the Zinc Oxide-Electrolyte Interface. *Journal of the Physical Chemistry of Solids* **1960**, *14*, 155-161.
(4) Ravishankar, S.; Bisquert, J.; Kirchartz, T. Interpretation of Mott–Schottky plots of photoanodes for water splitting. *Chemical Science* **2022**, *13* (17), 4828-4837.
(5) Hankin, A.; Bedoya-Lora, F. E.; Alexander, J. C.; Regoutz, A.; Kelsall, G. H. Flat band potential determination: avoiding the pitfalls. *Journal of Materials Chemistry A* **2019**, *7* (45), 26162-26176.
(6) Gomes, W. P.; VanMaekelbergh, D. Spectroscopy at Semiconductor Electrodes: Review and Recent Developments. *Electrochimica Acta* **1996**, *41*, 967-973.
(7) Garrett, C. G. B. Physical Theory of Semiconductor Surfaces. *Phys. Rev.* **1955**, *99*, 376-387.
(8) Shockley, W. The Theory of p-n Junctions in Semiconductors and p-n Junction Transistors. *Bell Sys. Tech. J.* **1949**, *28*, 435-489.
(9) Seiwatz, R.; Green, M. Space Charge Calculations for Semiconductors. *Journal of Applied Physics* **1958**, *29* ((7)), 1034-1040.
(10) Many, A.; Goldstein, Y.; Grover, N. B. *Semiconductor Surfaces*; North-Holland Publishing Company; New York, Interscience Publishers, 1965.
(11) Koval, C. A.; Austermann, R. L. The Effects of Surface Energetics on the Cyclic Voltammetry of Metallocenes at Nonilluminated n - InP Electrodes. *Journal of The Electrochemical Society* **1985**, *132* (11), 2656.
(12) Allongue, P. a. C. J. N. a. H. d. V. C. a. O. F. Analysis of CapacitancePotential Measurements at the Silicon−Electrolyte Interface Revisited. *The Journal of Physical Chemistry C* **2007**, *111* (14), 5497-5499.
(13) Tardella, A.; Chazalviel, J.-N. Highly accumulated electron layer at a semiconductor/electrolyte interface. *Phys. Rev. B* **1985**, *32*, 2439-2448.
(14) Gerischer, H.; McIntyre, R. A study of the charge and potential distribution at the semiconductor/electrolyte interface for the condition of degeneracy. *The Journal of Chemical Physics* **1985**, *83* (3), 1363-1370.
(15) Turner, J. A.; Manassen, J.; Nozik, A. J. Photoelectrochemistry with p-Si electrodes: Effects of inversion. *Applied Physics Letters* **2008**, *37* (5), 488-491. DOI: 10.1063/1.91741 (acccessed 4/29/2023).
(16) Allen J. Bard and Larry R. Faulkner, Electrochemical Methods: Fundamentals and Applications, New York: Wiley, 2001, 2nd ed.
(17) Natarajan, A. a. O. G. a. S. P. C. The Potential Distribution at the Semiconductor/Solution Interface. *The Journal of Physical Chemistry B* **1998**, *102* (40), 7793-7799.

 